Front. Optoelectron. 2016, 9(2): 249–258
DOI 10.1007/s12200-016-0611-6

REVIEW ARTICLE

Vertical-cavity surface-emitting lasers with nanostructures for optical interconnects

Anjin LIU (✉)[1,2], Dieter BIMBERG[2,3]

1 Laboratory of Solid-State Optoelectronics Information Technology, Institute of Semiconductors, Chinese Academy of Sciences, Beijing 100083, China
2 Institute of Solid State Physics, Technische Universität Berlin, Hardenbergstrasse 36, 10623 Berlin, Germany
3 King Abdulaziz University, Jeddah, Kingdom of Saudi Arabia (KSA)

Abstract Optical interconnects (OIs) are the only solution to fulfil both the requirements on large bandwidth and minimum power consumption of data centers and high-performance computers (HPCs). Vertical-cavity surface-emitting lasers (VCSELs) are the ideal light sources for OIs and have been widely deployed. This paper will summarize the progress made on modulation speed, energy efficiency, and temperature stability of VCSELs. Especially VCSELs with surface nanostructures will be reviewed in depth. Such lasers will provide new opportunities to further boost the performance of VCSELs and open a new door for energy-efficient OIs.

Keywords optical interconnects (OIs), vertical-cavity surface-emitting laser (VCSEL), subwavelength grating, modulation speed, energy efficiency

1 Introduction

As more and more devices are connected to the Internet, Internet data traffic grows dramatically and demands increasing performance of data centers as shown in Fig. 1 [1]. Especially, cloud computing and big data analysis urge higher data-center performance. Similarly high-performance computers (HPCs) are of steadily increasing interest to provide new levels of computational capability for applications such as geophysical data processing, drug discovery, and climate modeling. The performance of the top 500 supercomputers increases by a factor of 10 every 4 years in the past 20 years [2], and it is predicted that supercomputers will reach above 1 exaflops/s in 2020, 20 times higher performance than the current top supercomputer (see Fig. 2). To realize the expected performance of future data centers and HPCs, more communication bandwidth is demanded. Optical interconnect (OI) technology has been proved to be a huge success in the long-distance communication, and has been also deployed in short-reach applications in data centers and HPCs to replace copper-based electrical interconnects [3–8]. Compared with electrical interconnects, OIs have many advantages, for example, broad band, high density, small size, low loss, high power efficiency, and low crosstalk [8–10]. Currently OIs in Datacom and Computercom have been based on multi-mode fibers and vertical-cavity surface-emitting laser (VCSEL) technology, because of low cost, large alignment tolerance, ease of 2D array packaging, and high energy efficiency [11–15]. The wavelength of 850 nm for VCSEL-based links is applied in today's optical links in Datacom and Computercom, and recently the wavelength range from 900 to 1100 nm and even longer wavelengths is of growing interest [16–26]. This is because there are a large potential for higher speed and efficiency, improved reliability, improved dispersion, higher photodetector responsivity, and backside emission.

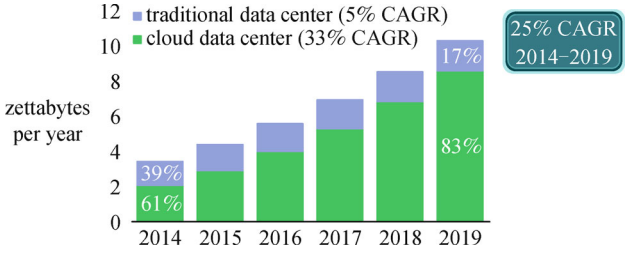

Fig. 1 Global data center IP traffic growth at a compound annual growth rate (CAGR) of 25% from 2014 to 2019 [1]

Received January 21, 2016; accepted February 1, 2016

E-mail: liuanjin@semi.ac.cn

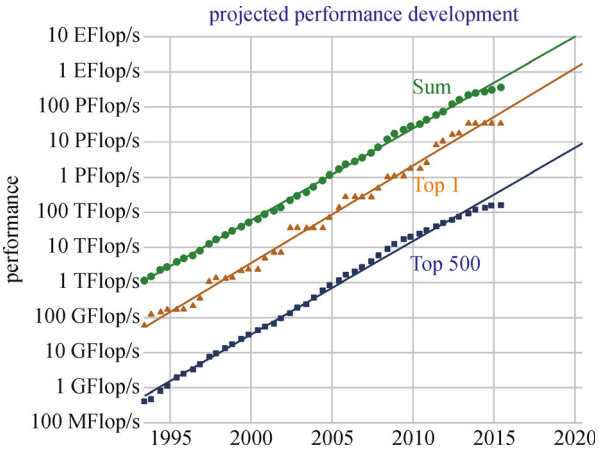

Fig. 2 Exponential growth of supercomputing power as recorded by the TOP500 list [2]

For VCSELs applied in OIs, high speed modulation is an essential requirement to meet the thirsty for permanently increasing bandwidth. As demands for network bandwidth exponentially increase, the size of data centers and HPCs becomes larger and more power is consumed. On the other hand, the heat dissipation in the systems leads to an operating environment for the optical components reaching temperatures of 85°C, even with advanced cooling technologies. Therefore, the VCSELs must be very energy-efficient, and be capable to maintain a high modulation speed at high temperatures without adjusting the operating parameters. In the past few years, VCSELs have achieved numerous and exciting successes in modulation speed, energy efficiency, and temperature stability [20–34]. To further boost the performance of VCSELs for OIs, adopting surface nanostructures to construct nano-scale VCSEL structures is one promising approach. This approach is expected not only to improve the modulation speed, energy efficiency, and temperature stability, but also to realize new functions and can be integrated with planar optical circuits to realize on-chip OIs. In this paper, first the dynamics of VCSELs will be briefly introduced. Then, some basic physics of nanostructures will be given. Finally, the progress of VCSELs with nanostructures will be reviewed, followed by a conclusion.

2 VCSELs for OIs

2.1 Dynamics of VCSELs

The dynamical behavior of semiconductor lasers is commonly described in terms of the rate equations [35]. The modulation speed of a VCSEL is limited by the intrinsic damping, self-heating, and external parasitics. The intrinsic modulation response of semiconductor lasers can be expressed as the transfer function

$$H_{\mathrm{i}}(f) = A \times \frac{f_{\mathrm{r}}^2}{f_{\mathrm{r}}^2 - f^2 + \mathrm{j}\frac{f}{2\pi}\gamma}, \tag{1}$$

where A is a constant, f_{r} the relaxation resonance frequency and γ the damping factor.

The relaxation resonance frequency is the oscillation frequency between the carriers and photons through the stimulated emission in the laser cavity. To achieve a high bandwidth, a VCSEL should reach a large relaxation resonance frequency. The relaxation resonance frequency increases with the bias current and can be formulated as

$$f_{\mathrm{r}} = D\sqrt{I - I_{\mathrm{th}}}, \tag{2}$$

with $D = \frac{1}{2\pi}\sqrt{\frac{\eta_{\mathrm{i}}\Gamma v_{\mathrm{g}}}{qV_{\mathrm{a}}} \times \frac{\partial g}{\partial n}}{\chi}$, where I_{th} is the threshold current, Γ the optical confinement factor, η_{i} the internal quantum efficiency, v_{g} the photon group velocity, V_{a} the active region volume, $\partial g/\partial n$ the differential gain, and χ the transport factor.

The damping factor is also a limit to achieve a high bandwidth besides the relaxation resonance frequency. The damping factor increases with the increase of the relaxation resonance frequency and is given as following equation

$$\gamma = Kf_{\mathrm{r}}^2 + \gamma_0,\ K = 4\pi^2\left(\tau_{\mathrm{p}} + \frac{\varepsilon\chi}{v_{\mathrm{g}}\frac{\partial g}{\partial n}}\right), \tag{3}$$

where τ_{p} is the photon lifetime and ε is the gain compression factor. The damping offset γ_0 is inversely proportional to the differential carrier lifetime.

To achieve a high bandwidth of VCSLs, a large D-factor and reasonable low K-factor are preferred, i.e., high differential gain [21–32], low photon lifetime [17,25,26, 36,37], and high confinement factor [25,26,33,37]. In the real devices, the relaxation resonance frequency and damping factor do not linearly increase with $\sqrt{I - I_{\mathrm{th}}}$ and f_{r}^2, respectively, because of thermal effects [12].

2.2 State of the art of VCSELs for OIs

For a high differential gain, compressively strained InGaAs quantum wells (QWs) are commonly employed in the wavelength range from 850 to 1200 nm [11–18,20–24]. Shallow surface etching has been adopted to tune the photon lifetime to enhance the modulation bandwidth but introduces mirror losses as shown in Fig. 3 [36]. However, Bimberg's group at TU Berlin experimentally showed that a short laser cavity, for example, $\lambda/2$-cavity, can greatly enhance the confinement factor to 5.1% from 3% in a $3\lambda/2$-cavity without degrading other parameters [37,38]. Figure 4 shows that there is a maximum peak of the field intensity distribution at the QWs region for the $\lambda/2$-cavity compared

with the $3\lambda/2$-cavity. At the same time, a short cavity means a low photon lifetime resulting in a low K-factor [37]. The reported highest speed of 71 Gbps for VCSELs was achieved with a $\lambda/2$-cavity [17]. For the energy efficiency, Bimberg's group reported the record lowest energy efficiency of 56 fJ/bit dissipated energy with a 3.5-μm VCSEL, as shown in Fig. 5 [28]. It has been shown that a small oxide aperture help to achieve a high energy efficiency because of the single mode operation and large mode spacing [28,33,34]. To improve the temperature stability, the wavelength of the laser cavity resonance is detuned from the gain peak wavelength in the laser design [39]. The gain peak has a shift rate of 0.396 nm/K for $In_{0.21}Ga_{0.79}As/GaAs_{0.88}P_{0.12}$ QW system, whereas the cavity resonance wavelength shifts to longer wavelengths with a rate of 0.061 nm/K. Thus the cavity resonance wavelength is positioned at the longer wavelength side of the gain curve at room temperature in the design, as shown in Fig. 6(a). Figure 6(b) shows that at 85°C error-free data transmission at 46 Gbit/s has been achieved for 980-nm VCSELs [31], and 50 Gb/s error-free data transmission at 90°C for 850-nm VCSELs [32].

3 VCSELs with HCGs

To push the performance of current VCSELs for OIs to a high level, nanostructures like high-contrast subwavelength gratings (HCGs) can be integrated to VCSELs due to the unique physics. Here we focus on one-dimensional (1D) HCGs. Two-dimensional (2D) HCGs (also called photonic crystal slabs) also can serve as broadband reflectors based on Fano resonance, and have been comprehensively reviewed elsewhere [40].

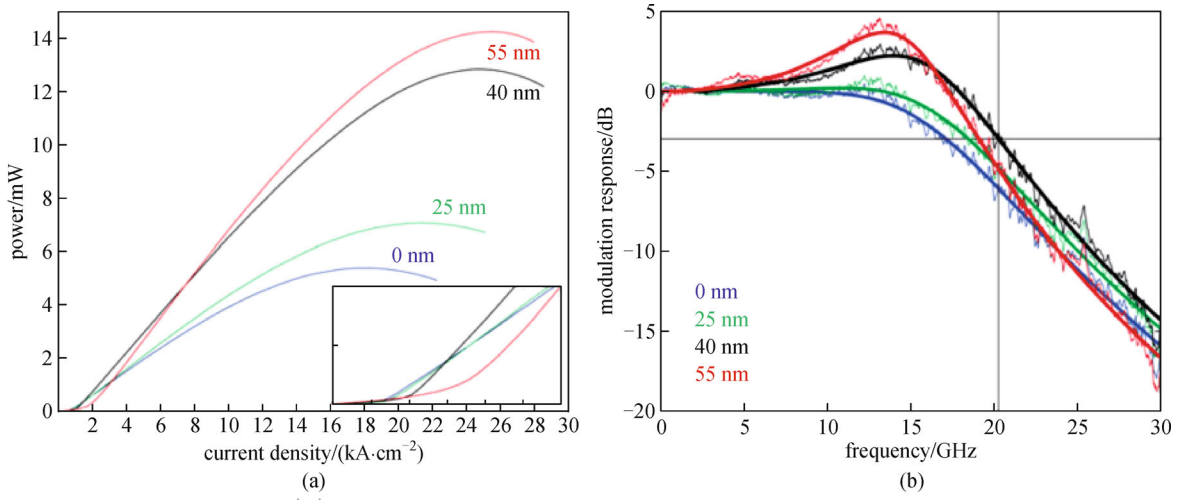

Fig. 3 (a) Output optical power versus current density for 11-μm oxide aperture VCSELs with different etch depths at 25°C. Inset: close-up of the threshold region; (b) measured small-signal modulation response at currents for maximum bandwidth for 11-μm oxide aperture VCSELs with different etch depths at 25°C [36]

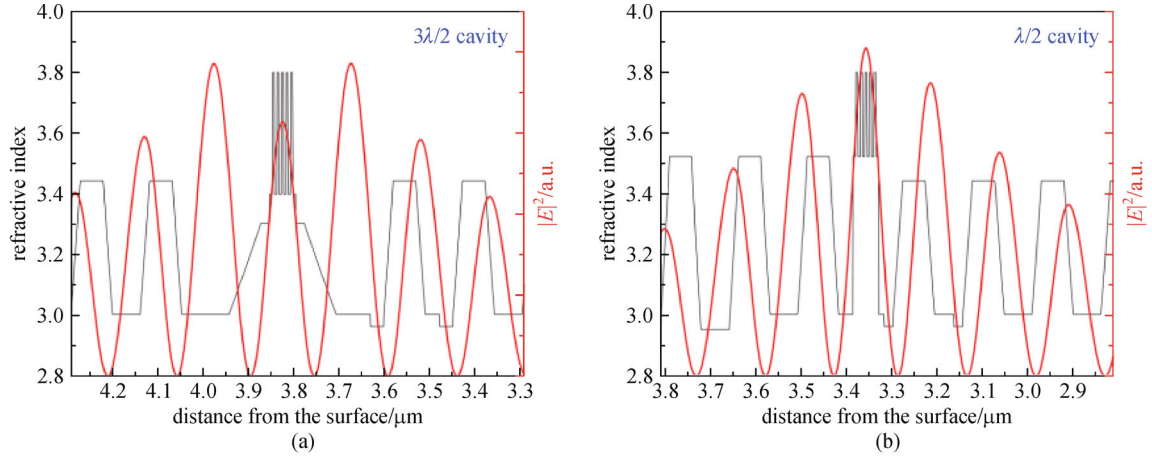

Fig. 4 Comparison of the refractive index and simulated optical field intensity distribution inside the previous VCSEL structure with a $3\lambda/2$ cavity (a) and inside the new VCSEL structure with a $\lambda/2$ cavity (b) [37]

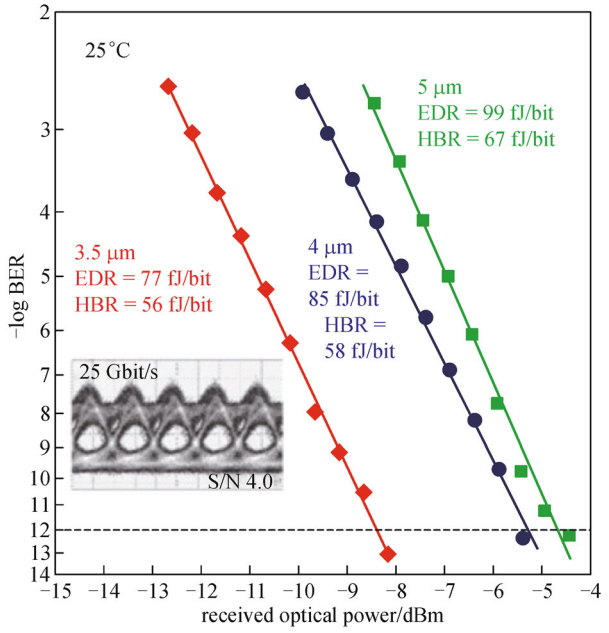

Fig. 5 BER against received optical power of VCSELs with oxide-aperture diameters of 3.5, 4, and 5 μm operating at 25 Gbit/s at bias currents yielding maximum energy efficiency [28]. BER: bit error ratio; EDR: energy-to-data ratio; HBR: heat-to-bit rate ratio

3.1 Physics of HCG reflector for VCSELs

HCG reflectors are also termed as photonic crystal mirrors or guided-mode resonant reflectors [41–47]. The grating bars composed of the high-index material in the HCG are fully immersed in the low-index medium, e.g., air, resulting in a high index contrast. The grating period is in the near-wavelength regime, between the wavelengths in the high-index material and in the low-index material. Figure 7 that shows the first two waveguide array modes with real propagation constants in infinite HCGs have a π-phase difference at the output plane and cancel each other causing a nearly 100% reflection [48]. When the first two modes are very closely located in the spectrum, a high-reflectivity broad band is realized [48]. There are other explanations for the high-reflectivity broad band of HCGs based on the Fano resonance or guided-mode resonance [43–47]. Thus, a broadband and high-reflectivity HCG can serve as a reflector and replace a part or full of the top distributed Bragg reflector (DBR) to construct a HCG-VCSEL [41–55]. Experimentally, HCG-VCSELs show a good mode selectivity and polarization control even for large oxide apertures [52–57].

For the HCG design, the structure parameters can be optimized by rigorous coupled wave analysis (RCWA) [58] and analytical methods [48]. These two methods consider that HCGs are with an infinite size and the incident wave is an infinite plane wave. The infinite-size HCG model is useful to rapidly search the parameters of HCGs. However, in the real devices the reflectivity is reduced caused by the finite HCG size [59], which increases the threshold current causing a low energy efficiency of VCSELs. Especially, the finite-size incident wave can excite the guided modes in the HCG by the higher-order angular components. The excited guided mode reduces the reflectivity and enhances the transmission as shown in Fig. 8(a) [60]. On the other hand, the excited guided mode can redirect the incident wave into the in-plane direction (see Fig. 8(b)), which provides the chances for the integrated optical sensor and for integration with planar optical circuits [61,62]. Therefore, it is indispensable to calculate the finite-size HCG by finite difference time domain method after choosing HCG

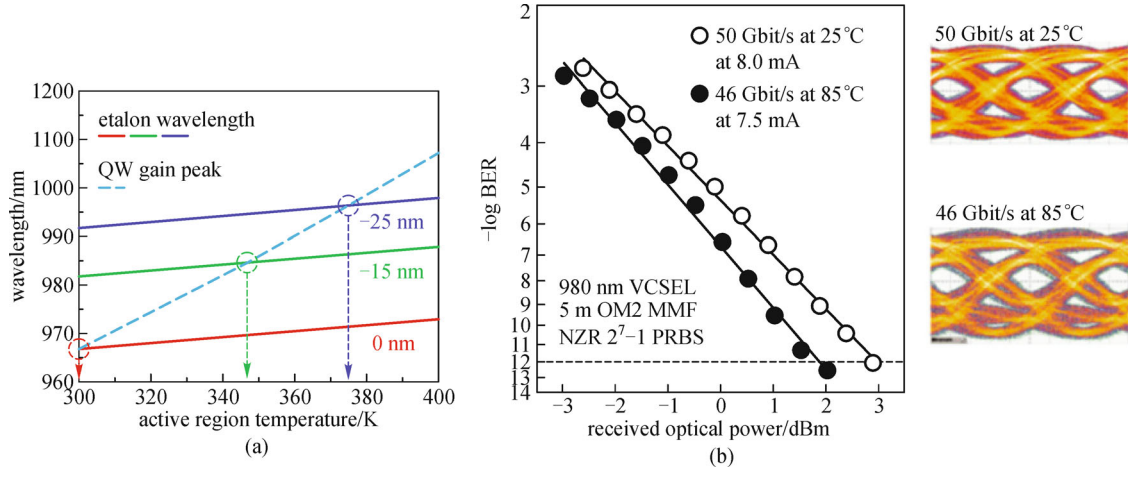

Fig. 6 (a) Peak gain wavelength of a single $In_{0.21}Ga_{0.79}As/GaAs_{0.88}P_{0.12}$ QW/barrier active region and the etalon resonance wavelength of our 980 nm VCSEL versus temperature for gain-to-etalon wavelength offsets fixed at 300 K at 0, – 15, and – 25 nm relative to the peak QW gain [39]; (b) large-signal modulation measurements of multimode oxide-confined 980 nm VCSEL at 50 and 46 Gbit/s at 25°C and 85°C, respectively [31]. OM2: optical mode 2; MMF: multimode fiber; NZR: non-return-to-zero; PBRS: pseudo random binary sequence

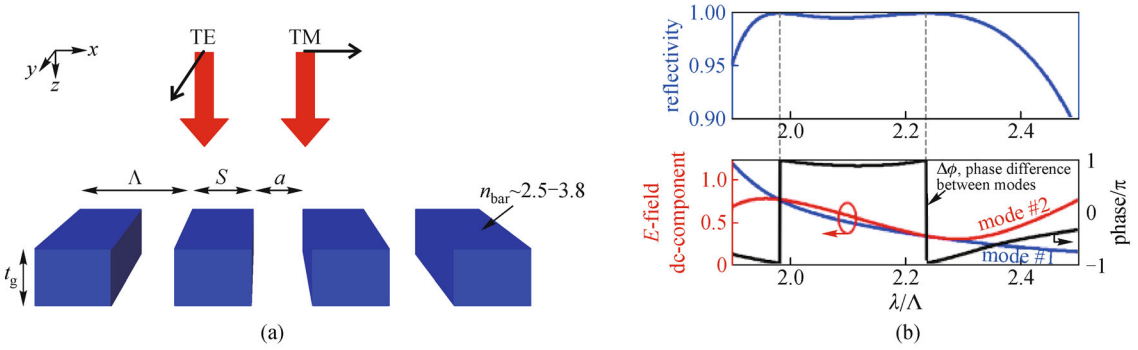

Fig. 7 (a) Schematic of the HCG; (b) double-mode solution exhibiting perfect cancellation at the HCG output plane leading to 100% reflectivity [48]. Λ: grating period; *S*: width of the grating bar; *a*: width of the air gap; TE: transverse electric; TM: transverse magnetic

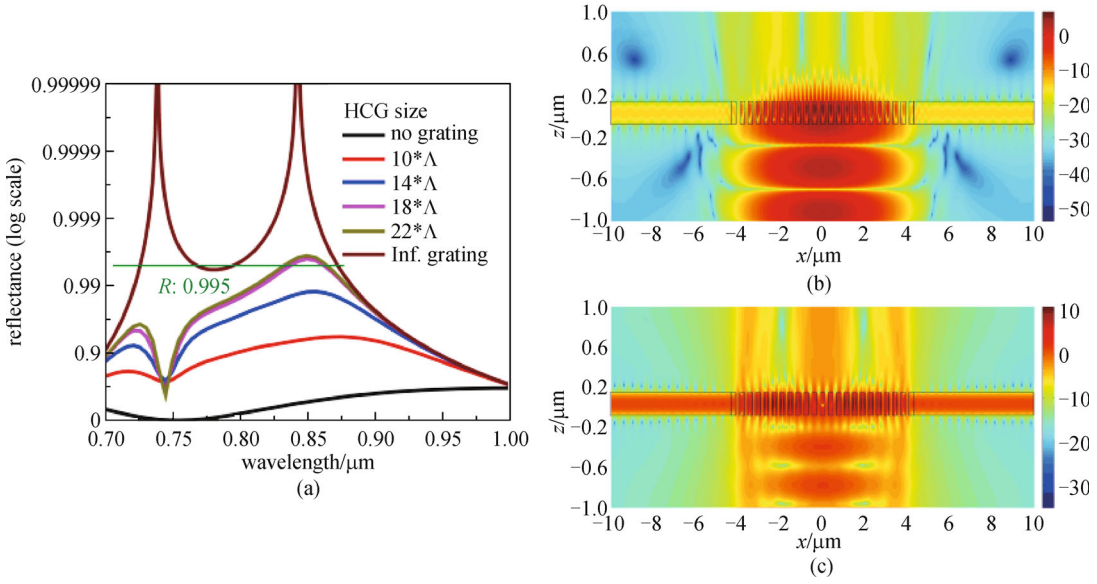

Fig. 8 (a) Reflectivity spectra for different HCG sizes with a fixed-size (4 μm, 1/e width of the Gaussian source) Gaussian source under normal incidence [60]; (b) mode field in finite-size HCG with a 4-μm Gaussian incident wave [61]; (c) guided mode with even symmetry with a 4-μm Gaussian incident wave [61]

parameters using RCWA or analytical methods in designing HCG reflector.

HCGs also show a strong ability to confine the field besides the feature of the high-reflectivity broad band. The energy penetration length of HCGs is much smaller than that of DBRs as shown in Fig. 9 [63]. The low energy penetration length brings a large confinement factor [64]. The small mode volume is very helpful to enhance the Purcell factor to reduce the carrier lifetime for a larger available modulation bandwidth and higher energy efficiency [32,33]. In HCGs, the phase penetration length related to the photon lifetime can be tuned by the structure parameters without degrading the reflectivity, not like the shallow surface etching method [36,65]. Thus due to the enlarged confinement factor in HCG-VCSELs and the optimum photon lifetime with a high reflectivity introduced by HCGs to VCSELs, HCG-VCSELs are expected to achieve a high relaxation resonance frequency, low damping factor, and low threshold current, which is very helpful for high-speed modulation and energy-efficient operation.

3.2 Progress of HCG-VCSELs

The first electrical HCG-VCSEL was realized with a sub-milliampere threshold current and single-mode and polarization-selective operation at 850 nm range as shown in Fig. 10 [52]. Later 1060-nm and 1550-nm HCG-VCSELs were developed [55,56]. Also tunable HCG-VCSELs were developed for fast tuning because of the compact HCG mirrors [53]. The maximum $f_{-3\,\mathrm{dB}}$ bandwidth is 7.8 GHz, which is limited by the parasitic

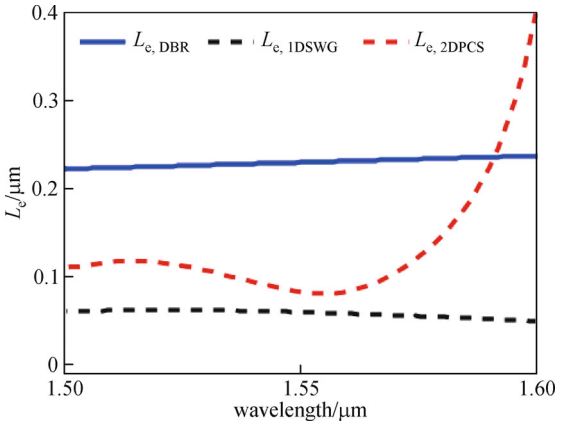

Fig. 9 Energy penetration depths for HCG, 2D photonic crystal slab, and DBR [63]

capacitance, and an error-free data transmission at 10 Gb/s was demonstrated at 1550 nm [66].

HCG reflectors are a kind of resonant structures, very different from DBRs, and the reflection phase can be tuned while keeping a high reflectivity [65]. By adjusting the HCG parameters like period and duty cycle, different wavelengths of HCG-VCSELs on a single wafer can be simultaneously achieved [67]. Therefore, HCG-VCSEL array with multiple uniformly spaced wavelengths can be constructed on a single HCG-VCSEL wafer for wavelength-division multiplexing (WDM) which provides a promising way to increase the aggregate bandwidth of a single fiber. Optically pumped HCG-VCSEL arrays were reported with double silicon-based HCGs as reflectors for dense WDM at 1.55 μm [68]. A GaAs-based HCG filter array with different resonance wavelengths were demonstrated targeting the application in electrically pumped

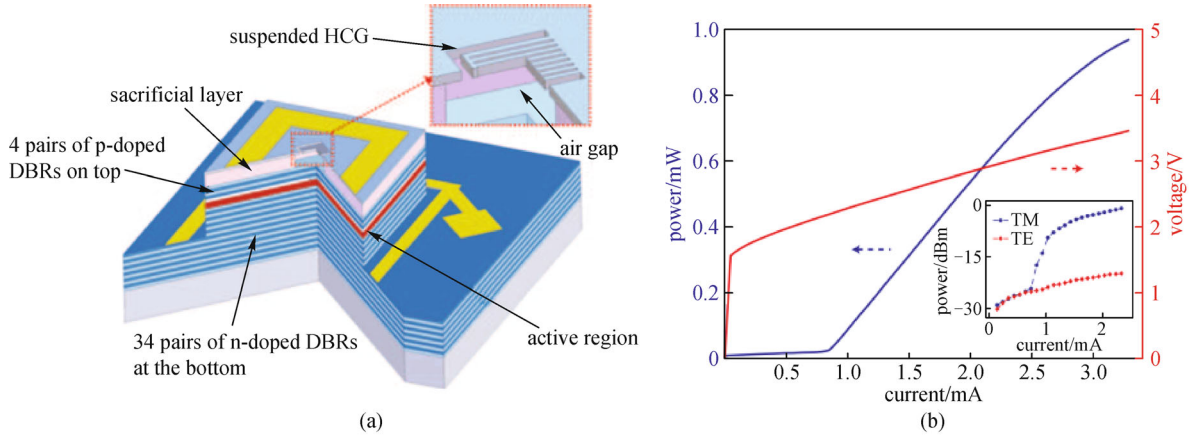

Fig. 10 Schematic of a HCG-VCSEL; (b) power-current-voltage curve of a HCG-VCSEL. The inset shows the polarization-resolved output power plotted in dB scale [52]

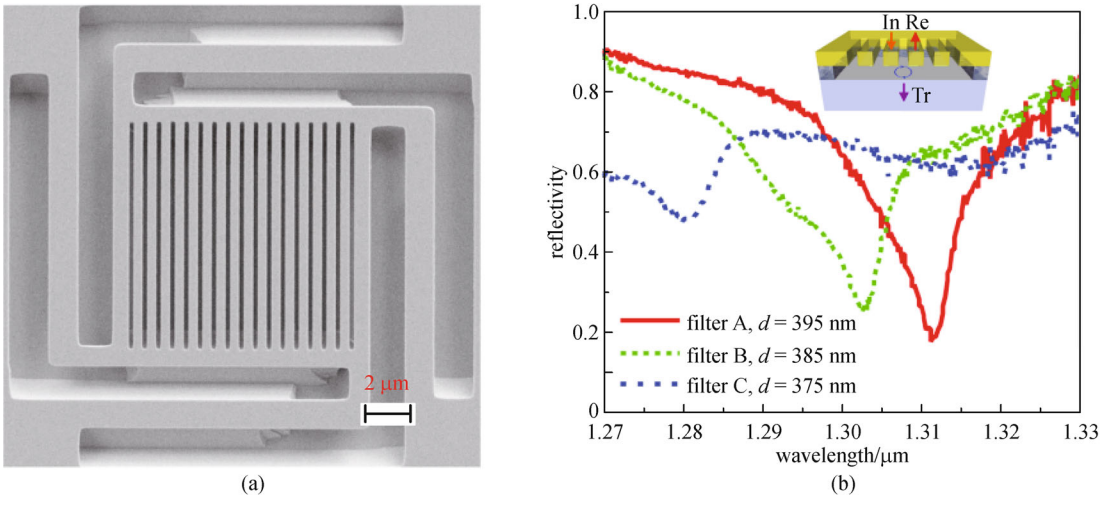

Fig. 11 (a) Scanning electronic microscopy (SEM) image of GaAs-based HCG; (b) reflectivity spectra of HCG-based filter array [69]

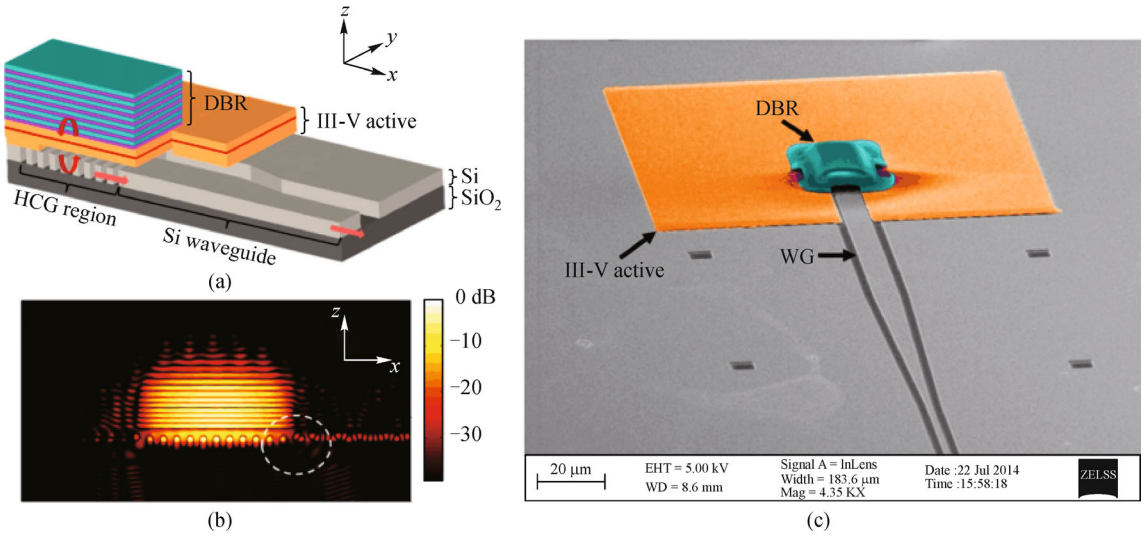

Fig. 12 (a) Schematic of the Si-VCSEL; (b) fundamental mode profile of the Si-VCSEL; (c) SEM image of the Si-VCSEL sample seen from the top [78]

HCG-VCSEL arrays as shown in Fig. 11 [69]. SiN-based HCGs were developed for WDM at 850 nm [70].

VCSELs have been the most successful light sources for short-reach interconnects, from ~1 m for module-to-module interconnects to several hundred meters for rack-to-rack interconnects. For future very-short-reach (meters to centimeters), ultrashort-reach (centimeters to millimeters), and even on-chip OIs, VCSELs are still promising light sources because of high energy efficiency, high modulation speed even at 85°C with a low thermal resistance. Thus one ongoing effort is to integrate VCSELs with planar optical circuits. Several approaches have been proposed and demonstrated like using 45° gold mirror [71] and grating coupler [72] for conventional VCSELs integrated with waveguides in the package level. These optical structures can transfer the vertical emitting light into the in-plane waveguides. Integrating a VCSEL structure with a waveguide in the design or fabrication phase makes the chip more compact. Inserting a diffraction grating into the top or bottom DBR can extract power to the in-plane waveguide [73,74]. Vertical coupling was also proposed to extract light from a FP microcavity composed of double HCG mirrors to a Si waveguide [75]. Very recently, HCGs have been proposed to replace the DBR as reflectors, and at the same time to route the emitting light into the in-plane waveguides [76,77]. This approach also brings a low thermal resistance for the devices. Figure 12 shows an optically-pumped hybrid vertical-cavity laser with lateral emission into a silicon waveguide using a silicon HCG at 1.5 μm [78]. The potential modulation speed was predicted up to 100 Gbit/s. For the short wavelength range, SiN-based HCGs were proposed to serve as reflectors and extract the light into the in-plane SiN waveguide because SiN is transparent from 600 to 1100 nm [70].

4 Conclusions and prospects

VCSELs for high-speed and energy-efficient optical links progress rapidly, and numerous achievements have been made in the past few years. VCSELs will continue to be the dominant light sources for Datacom, Computercom, and consumer links including short-reach OIs, and penetrate chip-to-chip and even on-chip OIs. Worldwide research from academic institutions as well as industrial companies is continuing to make efforts to enhance the energy efficiency, modulation speed, and temperature stability. Nanostructures with unique properties will play a critical role here. Future research in the areas of fundamental physics, new structures, and new technology will lead VCSELs to bit rates of >100 Gb/s at room temperature or even at 85°C, and an energy efficiency of <10 fJ/bit.

Acknowledgements We gratefully acknowledge the German Research Foundation (DFG) for funding via the collaborative research center 787 and the Alexander von Humboldt Foundation for supporting Anjin Liu by a Postdoctoral Research Fellowship. We thank W. Hofmann, G. Larisch, Hui Li, J. A. Lott, P. Moser, and P. Wolf for helpful discussion. Anjin Liu also gratefully acknowledges the support from Chinese Academy of Sciences (CAS) Pioneer Hundred Talents Program.

References

1. Cisco. Cisco Global Cloud Index: Forecast and Methodology, 2014–2019 White Paper, http://www.cisco.com/c/en/us/solutions/collateral/service-provider/global-cloud-index-gci/Cloud_Index_White_Paper.html
2. TOP500 supercomputer list of November 2015, http://www.top500.org/statistics/perfdevel/
3. Savage N. Linking with light. IEEE Spectrum, 2002, 39(8): 32–36
4. Benner A F, Ignatowski M, Kash J A, Kuchta D M, Ritter M B.

Exploitation of optical interconnects in future server architectures. IBM Journal of Research and Development, 2005, 49(4/5): 755–775
5. Coteus P W, Knickerbocker J U, Lam C H, Vlasov Y A. Technologies for exascale systems. IBM Journal of Research and Development, 2011, 55(5): 14-1–14-12
6. Lam C F, Liu H, Koley B, Zhao X, Kamalov V, Gill V. Fiber optic communication technologies: what's needed for datacenter network operations. IEEE Communications Magazine, 2010, 48(7): 32–39
7. Borkar S. Role of interconnects in the future of computing. Journal of Lightwave Technology, 2013, 31(24): 3927–3933
8. Taubenblatt M A. Optical interconnects for high-performance computing. Journal of Lightwave Technology, 2012, 30(4): 448–457
9. Miller D A B. Device requirements for optical interconnects to silicon chips. Proceedings of the IEEE, 2009, 97(7): 1166–1185
10. Miller D A B. Rationale and challenges for optical interconnects to electronic chips. Proceedings of the IEEE, 2000, 88(6): 728–749
11. Bimberg D. Ultrafast VCSELs for Datacom. IEEE Photonics Journal, 2010, 2(2): 273–275
12. Larsson A. Advances in VCSELs for communication and sensing. IEEE Journal of Selected Topics in Quantum Electronics, 2011, 17 (6): 1552–1567
13. Tatum J A, Gazula D, Graham L A, Guenter J K, Johnson R H, King J, Kocot C, Landry G D, Lyubomirsky I, MacInnes A N, Shaw E M, Balemarthy K, Shubochkin R, Vaidya D, Yan M, Tang F. VCSEL-based interconnects for current and future data centers. Journal of Lightwave Technology, 2015, 33(4): 727–732
14. Grabherr M, Intemann S, King R, Wabra S, Jäger R, Riedl M. VCSEL arrays for high aggregate bandwidth of up to 1.34 Tbps. Proceedings of the Society for Photo-Instrumentation Engineers, 2014, 9001: 900105-1–900105-10
15. Michalzik R. VCSELs-Fundamentals, Technology and Applications of Vertical-Cavity Surface-Emitting Lasers. Berlin: Springer, 2013, 166
16. Blokhin S A, Lott J A, Mutig A, Fiol G, Ledentsov N N, Maximov M V, Nadtochiy A M, Shchukin V A, Bimberg D. Oxide-confined 850 nm VCSELs operating at bit rates up to 40 Gbit/s. Electronics Letters, 2009, 45(10): 501–503
17. Kuchta D, Rylyakov A, Doany F E, Schow C, Proesel J, Baks C, Westbergh P, Gustavsson J, Larsson A A. 71 Gb/s NRZ modulated 850 nm VCSEL-based optical link. IEEE Photonics Technology Letters, 2015, 27(6): 577–580
18. Shi J W, Wei Z R, Chi K L, Jiang J W, Wun J M, Lu I C, Chen J, Yang Y J. Single-mode, high-speed, and high-power vertical-cavity surface-emitting lasers at 850 nm for short to medium reach (2 km) optical interconnects. Journal of Lightwave Technology, 2013, 31 (24): 4037–4044
19. Hanson D. Case for using 980 nm (rather than 850 nm) VCSELs for serial 10 Gb/s links with new higher-bandwidth 50 MMF.1999 [Online]. http://www.ieee802.org/3/10G_study/public/july99/hanson_1_0799.pdf
20. Chang Y C, Coldren L A. Efficient, high-data-rate, tapered oxide-aperture vertical-cavity surface-emitting lasers. IEEE Journal of Selected Topics in Quantum Electronics, 2009, 15(3): 704–715
21. Mutig A, Lott J A, Blokhin S A, Wolf P, Moser P, Hofmann W, Nadtochiy A M, Payusov A, Bimberg D. Highly temperature-stable modulation characteristics of multioxide-aperture high-speed 980 nm vertical cavity surface emitting lasers. Applied Physics Letters, 2010, 97(15): 151101
22. Wolf P, Moser P, Larisch G, Hofmann W, Bimberg D. High-speed and temperature-stable, oxide-confined 980 nm VCSELs for optical interconnects. IEEE Journal of Selected Topics in Quantum Electronics, 2013, 19(4): 1701207
23. Héroux J B, Kise T, Funabashi M, Aoki T, Schow C L, Rylyakov A V, Nakagawa S. Energy-efficient 1060-nm optical link operating up to 28 Gb/s. Journal of Lightwave Technology, 2015, 33(4): 733–740
24. Hatakeyama H, Anan T, Akagawa T, Fukatsu K, Suzuki N, Tokutome K, Tsuji M. Highly reliable high-speed 1.1-μm-range VCSELs with InGaAs/GaAsP-MQWs. IEEE Journal of Quantum Electronics, 2010, 46(6): 890–897
25. Müller M, Wolf P, Gründl T, Grasse C, Rosskopf J, Hofmann W, Bimberg D, Amann M C. Energy-efficient 1.3 m short-cavity VCSELs for 30 Gb/s error-free optical links. In: Proceedings of 23rd Semiconductor Laser Conference (ISLC), 2012, 1–2
26. Müller M, Hofmann W, Gründl T, Horn M, Wolf P, Nagel R D, Rönneberg E, Böhm G, Bimberg D, Amann M C. 1550-nm high-speed short-cavity VCSELs. IEEE Journal of Selected Topics in Quantum Electronics, 2011, 17(5): 1158–1166
27. Moser P, Hofmann W, Wolf P, Lott J A, Larisch G, Payusov A S, Ledentsov N N, Bimberg D. 81 fJ/bit energy-to-data ratio of 850 nm vertical-cavity surface-emitting lasers for optical interconnects. Applied Physics Letters, 2011, 98(23): 231106
28. Moser P, Lott J A, Wolf P, Larisch G, Li H, Ledentsov N N, Bimberg D. 56 fJ dissipated energy per bit of oxide-confined 850 nm VCSELs operating at 25 Gbit/s. Electronics Letters, 2012, 48(20): 1292–1294
29. Haglund E, Westbergh P, Gustavsson J S, Haglund E P, Larsson A, Geen M, Joel A. 30 GHz bandwidth 850 nm VCSEL with sub-100 fJ/bit energy dissipation at 25–50 Gbit/s. Electronics Letters, 2015, 51(14): 1096–1098
30. Li H, Wolf P, Moser P, Larisch G, Mutig A, Lott J A, Bimberg D. Energy-efficient and temperature-stable oxide-confined 980 nm VCSELs operating error-free at 38 Gbit/s at 85°C. Electronics Letters, 2014, 50(2): 103–105
31. Moser P, Lott J A, Wolf P, Larisch G, Li H, Bimberg D. Error-free 46 Gbit/s operation of oxide-confined 980 nm VCSELs at 85°C. Electronics Letters, 2014, 50(19): 1369–1371
32. Kuchta D M, Rylyakov A V, Schow C L, Proesel J E, Baks C W, Westbergh P, Gustavsson J S, Larsson A A. 50 Gb/s NRZ modulated 850 nm VCSEL transmitter operating error free to 90°C. Journal of Lightwave Technology, 2015, 33(4): 802–810
33. Tan F, Wu C H, Feng M, Holonyak N Jr. Energy efficient microcavity lasers with 20 and 40 Gb/s data transmission. Applied Physics Letters, 2011, 98(19): 191107
34. Wu C H, Tan F, Feng M, Holonyak N Jr. The effect of mode spacing on the speed of quantum-well microcavity lasers. Applied Physics Letters, 2010, 97(9): 091103
35. Coldren L A, Corzine S W. Diode Lasers and Photonic Integrated Circuits. New York: Wiley, 1995
36. Westbergh P, Gustavsson J S, Kögel B, Haglund Å, Larsson A. Impact of photon lifetime on high-speed VCSEL performance. IEEE Journal of Selected Topics in Quantum Electronics, 2011, 17(6):

1603–1613
37. Mutig A, Bimberg D. Progress on high-speed 980nm VCSELs for short-reach optical interconnects. Advances in Optical Technologies, 2011, 2011: 290508
38. Moser P, Wolf P, Mutig A, Larisch G, Unrau W, Hofmann W, Bimberg D. 85°C error-free operation at 38 Gb/s of oxide-confined 980-nm vertical-cavity surface-emitting lasers. Applied Physics Letters, 2012, 100(8): 081103
39. Li H, Wolf P, Moser P, Larisch G, Mutig A, Lott A, Bimberg D H. Impact of the quantum well gain-to-cavity etalon wavelength offset on the high temperature performance of high bit rate 980-nm VCSELs. IEEE Journal of Quantum Electronics, 2014, 50(8): 613–621
40. Zhou W, Zhao D, Shuai Y C, Yang H, Chuwongin S, Chadha A, Seo J H, Wang K X, Liu V, Ma Z, Fan S. Progress in 2D photonic crystal Fano resonance photonics. Progress in Quantum Electronics, 2014, 38(1): 1–74
41. Mateus C F R, Huang M C Y, Deng Y, Neureuther A R, Chang-Hasnain C J. Ultrabroadband mirror using low-index cladded subwavelength grating. IEEE Photonics Technology Letters, 2004, 16(2): 518–520
42. Mateus C F R, Huang M C Y, Chen L, Chang-Hasnain C J, Suzuki Y. Broad-band mirror (1.12–1.62 μm) using a subwavelength grating. IEEE Photonics Technology Letters, 2004, 16(7): 1676–1678
43. Boutami S, Ben Bakir B, Leclercq J L, Letartre X, Rojo-Romeo P, Garrigues M, Viktorovitch P, Sagnes I, Legratiet L, Strassner M. Highly selective and compact tunable MOEMS photonic crystal Fabry-Perot filter. Optics Express, 2006, 14(8): 3129–3137
44. Sciancalepore C, Bakir B B, Letartre X, Fedeli J M, Olivier N, Bordel D, Seassal C, Rojo-Romeo P, Regreny P, Viktorovitch P. Quasi-3D light confinement in double photonic crystal reflectors VCSELs for CMOS-compatible integration. Journal of Lightwave Technology, 2011, 29(13): 2015–2024
45. Viktorovitch P, Bakir B B, Boutami S, Leclercq J L, Letartre X, Rojo-Romeo P, Seassal C, Zussy M, Cioccio L D, Fedeli J M. 3D harnessing of light with 2.5D photonic crystals. Laser & Photonics Reviews, 2010, 4(3): 401–413
46. Magnusson R, Shokooh-Saremi M. Physical basis for wideband resonant reflectors. Optics Express, 2008, 16(5): 3456–3462
47. Shokooh-Saremi M, Magnusson R. Wideband leaky-mode resonance reflectors: influence of grating profile and sublayers. Optics Express, 2008, 16(22): 18249–18263
48. Karagodsky V, Sedgwick F G, Chang-Hasnain C J. Theoretical analysis of subwavelength high contrast grating reflectors. Optics Express, 2010, 18(16): 16973–16988
49. Liu A, Fu F, Wang Y, Jiang B, Zheng W. Polarization-insensitive subwavelength grating reflector based on a semiconductor-insulator-metal structure. Optics Express, 2012, 20(14): 14991–15000
50. Debernardi P, Orta R, Gründl T, Amann M C. 3-D vectorial optical model for high-contrast grating vertical-cavity surface-emitting lasers. IEEE Journal of Quantum Electronics, 2013, 49(2): 137–145
51. Gębski M, Kuzior O, Dems M, Wasiak M, Xie Y Y, Xu Z J, Wang Q J, Zhang D H, Czyszanowski T. Transverse mode control in high-contrast grating VCSELs. Optics Express, 2014, 22(17): 20954–20963
52. Huang M C Y, Zhou Y, Chang-Hasnain C J. A surface-emitting laser incorporating a high-indexcontrast subwavelength grating. Nature Photonics, 2007, 1(2): 119–122
53. Huang M C Y, Zhou Y, Chang-Hasnain C J. A nanoelectromechanical tunable laser. Nature Photonics, 2008, 2(3): 180–184
54. Boutami S, Benbakir B, Leclercq J L, Viktorovitch P. Compact and polarization controlled 1.55 μm vertical-cavity surface emitting laser using single-layer photonic crystal mirror. Applied Physics Letters, 2007, 91(7): 071105
55. Hofmann W, Chase C, Müller M, Rao Y, Grasse C, Böhm G, Amann M C, Chang-Hasnain C J. Long-wavelength high-contrast grating vertical-cavity surface-emitting laser. IEEE Photonics Journal, 2010, 2(3): 415–422
56. Ansbæk T, Chung I S, Semenova E S, Yvind K. 1060-nm tunable monolithic high index contrast subwavelength grating VCSEL. IEEE Photonics Technology Letters, 2013, 25(4): 365–367
57. Inoue S, Kashino J, Matsutani A, Ohtsuki H, Miyashita T, Koyama F. Highly angular dependent high-contrast grating mirror and its application for transverse-mode control of VCSELs. Japanese Journal of Applied Physics, 2014, 53(9): 090306
58. Moharam M G, Gaylord T K. Rigorous coupled-wave analysis of planar grating diffraction. Journal of the Optical Society of America, 1981, 71(7): 811–818
59. Huang M C Y, Zhou Y, Chang-Hasnain C J. Single mode high-contrast subwavelength grating vertical cavity surface emitting lasers. Applied Physics Letters, 2008, 92(17): 171108
60. Liu A, Hofmann W, Bimberg D. Two dimensional analysis of finite size high-contrast gratings for applications in VCSELs. Optics Express, 2014, 22(10): 11804–11811
61. Liu A, Hofmann W, Bimberg D. Integrated high-contrast-grating optical sensor using guided mode. IEEE Journal of Quantum Electronics, 2015, 51(1): 1–8
62. Liu A, Hofmann W, Bimberg D. VCSELs with surface nanostructures. In: Proceedings of Asia Communications and Photonics Conference, 2014, ATh2B. 4
63. Zhao D, Ma Z, Zhou W. Field penetrations in photonic crystal Fano reflectors. Optics Express, 2010, 18(13): 14152–14158
64. Babic D I, Corzine S W. Analytic expressions for the reflection delay, penetration depth, and absorptance of quarter-wave dielectric mirrors. IEEE Journal of Quantum Electronics, 1992, 28(2): 514–524
65. Chung I S, Mørk J. Speed enhancement in VCSELs employing grating mirrors. Proceedings of the Society for Photo-Instrumentation Engineers, 2013, 8633: 863308
66. Rao Y, Yang W, Chase C, Huang M C Y, Worland D P, Khaleghi S, Chitgarha M R, Ziyadi M, Willner A E, Chang-Hasnain C J. Long-Wavelength VCSEL using high-contrast grating. IEEE Journal of Selected Topics in Quantum Electronics, 2013, 19(4): 1701311
67. Karagodsky V, Pesala B, Chase C, Hofmann W, Koyama F, Chang-Hasnain C J. Monolithically integrated multi-wavelength VCSEL arrays using high-contrast gratings. Optics Express, 2010, 18(2): 694–699
68. Sciancalepore C, Bakir B B, Menezo S, Letartre X, Bordel D, Viktorovitch P. III–V-on-Si photonic crystal vertical-cavity surface-emitting laser arrays for wavelength division multiplexing. IEEE Photonics Technology Letters, 2013, 25(12): 1111–1113

69. Liu A, Wolf P, Schulze J H, Bimberg D. Fabrication and characterization of integrable GaAs-based high-contrast grating reflector and Fabry-Pérot filter array with GaInP sacrificial layer. IEEE Photonics Journal, 2016, 8(1): 2700509
70. Kumari S, Gustavsson J S, Wang R, Haglund E P, Westbergh P, Sanchez D, Haglund E, Haglund Å, Bengtsson J, Thomas N L, Roelkens G, Larsson A, Baets R. Integration of GaAs-based VCSEL array on SiN platform with HCG. Proceedings of the Society for Photo-Instrumentation Engineers, 2015, 9372: 93720U-1–93720U-7
71. Schares L, Kash J A, Doany F E, Schow C L, Schuster C, Kuchta D M, Pepeljugoski P K, Trewhella J M, Baks C W, John R A, Shan L, Kwark Y H, Budd R A, Chiniwalla P, Libsch F R, Rosner J, Tsang C K, Patel C S, Schaub J D, Dangel R, Horst F, Offrein B J, Kucharski D, Guckenberger D, Hegde S, Nyikal H, Lin C K, Tandon A, Trott G R, Nystrom M, Bour D P, Tan M R T, Dolfi D W. Terabus: terabit/second-class card-level optical interconnect technologies. IEEE Journal of Selected Topics in Quantum Electronics, 2006, 12(5): 1032–1044
72. Kaur K S, Subramanian A Z, Cardile P, Verplancke R, Van Kerrebrouck J, Spiga S, Meyer R, Bauwelinck J, Baets R, Van Steenberge G. Flip-chip assembly of VCSELs to silicon grating couplers via laser fabricated SU8 prisms. Optics Express, 2015, 23 (22): 28264–28270
73. Louderback D A, Pickrell G W, Lin H C, Fish M A, Hindi J J, Guilfoyle P S. VCSELs with monolithic coupling to internal horizontal waveguides using integrated diffraction gratings. Electronics Letters, 2004, 40(17): 1064–1065
74. Haglund E P, Kumari S, Westbergh P, Gustavsson J S, Roelkens G, Baets R, Larsson A. Silicon-integrated short-wavelength hybrid-cavity VCSEL. Optics Express, 2015, 23(26): 33634–33640
75. Ferrier L, Romeo P R, Letartre X, Drouard E, Viktorovitch P. 3D integration of photonic crystal devices: vertical coupling with a silicon waveguide. Optics Express, 2010, 18(15): 16162–16174
76. Ferrara J, Yang W, Zhu L, Qiao P, Chang-Hasnain C J. Heterogeneously integrated long-wavelength VCSEL using silicon high contrast grating on an SOI substrate. Optics Express, 2015, 23 (3): 2512–2523
77. Chung I S, Mørk J. Silicon-photonics light source realized by III–V/Si-grating-mirror laser. Applied Physics Letters, 2010, 97(15): 151113
78. Park G C, Xue W, Taghizadeh A, Semenova E, Yvind K, Mørk J, Chung I S. Hybrid vertical-cavity laser with lateral emission into a silicon waveguide. Laser & Photonics Reviews, 2015, 9(3): L11–L15

Anjin Liu received the Bachelor degree in electronics of science and technology in 2006 from Huazhong University of Science and Technology, Wuhan, China, and Ph.D. degree in physical electronics from Institute of Semiconductors, Chinese Academy of Sciences (CAS), Beijing, in 2011, both with honors.

From 2006 to 2011, he was with Institute of Semiconductors, CAS, and was involved in the research on single-mode VCSELs with surface microstructures. From 2012 to July 2013, he was a Postdoc Fellow in Fraunhofer Heinrich Hertz Institute in Berlin, and worked on polymer OEIC. In August of 2013, he joined the group of Prof. Dieter H. Bimberg in Technische Universität Berlin, and explores surface emitters with surface nanostructures for high-speed modulation and new applications. In 2016, he is appointed as Associate Professor with CAS Pioneer Hundred Talents Program in Institute of Semiconductors, CAS. His research interests include modeling, fabricating, and characterizing passive and active photonic devices. He has authored or coauthored about 50 papers in scientific journals and conference proceedings, and holds 1 filed US patent and 12 issued Chinese patents.

He was the recipients of Special Prize of President Scholarship for Postgraduate Students, CAS (2011), Excellent Doctoral Dissertation Award, CAS (2012), and Alexander von Humboldt Postdoctoral Research Fellowship, Germany (2013).

Dieter H. Bimberg received the Diploma in physics and the Ph.D. degree from Goethe University, Frankfurt, in 1968 and 1971, respectively. From 1972 to 1979, he held a Principal Scientist position at the Max Planck-Institute for Solid State Research in Grenoble/France and Stuttgart. In 1979, he was appointed as Professor of Electrical Engineering, Technical University of Aachen.

In 1981, he was appointed to the Chair of Applied Solid State Physics at Technische Universität Berlin. He was elected in 1990 Excecutive Director of the Solid State Physics Institute at TU Berlin, a position he hold until 2011. In 2004, he founded the Center of Nanophotonics at TU Berlin. From 2006 to 2011, he was the chairman of the board of the German Federal Government Centers of Excellence in Nanotechnologies.

His honors include the Russian State Prize in Science and Technology 2001, his election to the German Academy of Sciences Leopoldina in 2004, to the Russian Academy of Sciences in 2011, and to the US National Academy of Engineering in 2014, as Fellow of the American Physical Society and IEEE in 2004 and 2010, respectively, the Max-Born-Award and Medal 2006, awarded jointly by IoP and DPG, the William Streifer Award of the Photonics Society of IEEE in 2010, the UNESCO Nanoscience Medal 2012, and the Heinrich-Welker-Award and medal in 2015. The University of Lancaster bestowed in 2015 the D.Sc.h.c. to him.

He has authored more than 1200 papers, 25 patents, and 6 books resulting in more than 48000 citations worldwide and a Hirsch factor of 98.

His research interests include the growth and physics of nanostructures and nanophotonic devices, ultrahigh speed and energy efficient photonic devices for future datacom systems, single/entangled photon emitters for quantum cryptography and ultimate nanomemories based on quantum dots.